

# Spatial Resolution Effects on Chlorophyll Fluorescence Retrieval in a Heterogeneous Canopy Using Hyperspectral Imagery and Radiative Transfer Simulation

Pablo J. Zarco-Tejada, Lola Suárez, and Victoria González-Dugo

**Abstract**—Increasing attention is being given to chlorophyll fluorescence (F) for global monitoring of vegetation due to its relationship with physiology. New progress has been made in the methodological and technical aspects of signal retrieval with the recently published low-resolution global maps of fluorescence. Nevertheless, little progress has been made in the interpretation of the F signal when quantified in large pixels, an important issue due to the effects of structure, percentage cover, shadows, and background. High-resolution (40 cm) airborne hyperspectral imagery is used in this letter to assess the retrieval of fluorescence by the Fraunhofer line depth method from pure tree crowns and aggregated pixels. Due to canopy heterogeneity, the F signal extracted from aggregated pixels is highly degraded. A poor relationship is obtained between fluorescence extracted from pure tree crowns ( $F_{\text{crown}}$ ) and that quantified from pixels aggregating pure tree crowns, shadows, and background ( $F_{\text{aggregated}}$ ) ( $R^2 = 0.25$ ;  $p < 0.01$ ). The relationship between F and stomatal conductance (used as a physiological indicator) decreases as a function of aggregation, yielding  $R^2 = 0.69$  ( $p < 0.01$ ) when calculated from pure tree crowns and  $R^2 = 0.38$  ( $p < 0.05$ ) from pixels containing crown, shadows, and soil. This letter demonstrates the need for methods to accurately retrieve a pure-vegetation fluorescence signal from aggregated pixels. The FluorMODleaf and FluorSAIL models were combined with the geometric forest light interaction model (FLIM) model and led to the “Fluor-FLIM” model developed for this letter. Simulations conducted with FluorFLIM obtain predictive relationships between  $F_{\text{crown}}$  and  $F_{\text{aggregated}}$  pixels as a function of percentage cover, enabling the estimation of pure-crown F from aggregated pixels ( $R^2 = 0.72$ ,  $p < 0.01$ ).

**Index Terms**—Canopy modeling, fluorescence, Fraunhofer line depth (FLD), heterogeneous, unmanned aerial vehicle (UAV).

Manuscript received July 5, 2012; revised December 12, 2012; accepted March 12, 2013. This work was supported by the Spanish Ministry of Science and Education under Project AGL2009-13105 and Project AGL2012-40053-C03-01, and CONSOLIDER RIDEKO (CSD2006-67).

P. J. Zarco-Tejada is with the Department of Remote Sensing, Spanish National Research Council, Cordoba 14004, Spain (e-mail: pzarco@ias.csic.es).

L. Suárez is with the School of Mathematical and Geospatial Sciences, RMIT University, Melbourne, Vic. 3001, Australia (e-mail: lola.suarezbarranco@rmit.edu.au).

V. González-Dugo is with the Department of Agronomy, Institute for Sustainable Agriculture, Spanish National Research Council, Cordoba 14004, Spain (e-mail: victoria.gonzalez@ias.csic.es).

Color versions of one or more of the figures in this paper are available online at <http://ieeexplore.ieee.org>.

Digital Object Identifier 10.1109/LGRS.2013.2252877

## I. INTRODUCTION

**I**N RECENT years, increasing attention has been given to chlorophyll fluorescence (F) for global monitoring of vegetation physiology. In particular, specific studies have explored the technical aspects and challenges of retrieving fluorescence to monitor global photosynthesis [1]. Recently, progress in F retrieval has focused on modeling. Several methods have been assessed for extracting the signal at leaf and canopy levels with very narrow spectral bands [2]–[6]. These methodological improvements have shown the feasibility of fluorescence retrieval using the  $O_2\text{-A}$  band feature at the proximal scales, from airborne hyperspectral imagers [7] and at the satellite level [8]. From a technical point of view, Damm *et al.* [9] explored the implications of relevant sensor properties on F retrieval accuracy. International efforts aim to launch a dedicated satellite sensor to monitor fluorescence from space for global studies. This objective can be reached at the medium resolution scale (i.e., hundreds of meters per pixel). In fact, the first global maps of F have recently been published [10], [11] using the TANSO sensor on board GOSAT [12], making qualitative assessments with annual and seasonal vegetation patterns [13]. Although these global maps of F are important achievements, questions are raised regarding the interpretation of F retrieved from mixed pixels of hundreds of meters that aggregate vegetation, soil, and shadow components. Studies conducted at very fine resolution would make it possible to assess the effects of canopy structure on the mixed F signal retrieved from aggregated pixels of soil, shadows, and canopy background components. Models currently available to simulate the effects of F on leaf and canopy radiance—particularly FluorMODleaf [14] and FluorSAIL [15]—are valid for homogeneous canopies. The lack of models to simulate F in heterogeneous canopies prevents progress in its interpretation when the F signal is quantified at coarse spatial resolutions.

Therefore, work needs to be conducted on the implications of pixel size on the quantified fluorescence signal, including shadows and background. Such efforts will help to better assess the impact of aggregations on physiological measures linked to fluorescence, such as photosynthesis. For the first time, this letter addressed the issue of the F signal of a mixed pixel, raising important questions on validity and

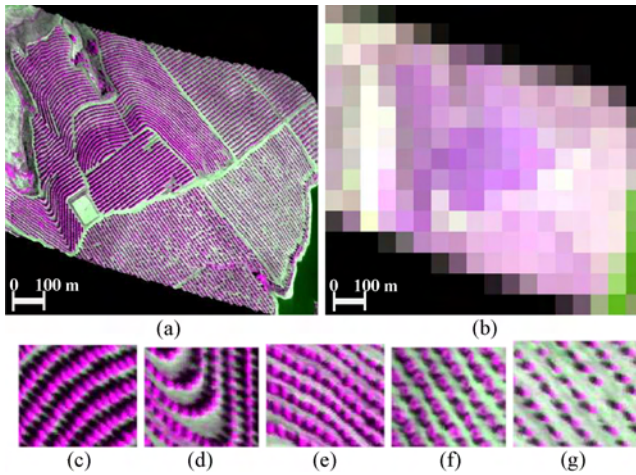


Fig. 1. (a) Airborne hyperspectral imagery acquired with the micro-Hyperspec VNIR sensor on board a UAV yielding 40-cm resolution. (b) Resampled to 50-m pixels to assess the aggregation effects on fluorescence retrieval. (c)–(g) Complexity of planting grids/orientations. Images are shown in color composites using green, red, and NIR bands.

interpretation. Its main focus was the assessment of chlorophyll fluorescence in aggregated pixels using very high-resolution airborne hyperspectral imagery, showing the implications of percentage cover and pixel components on the signal retrieved.

## II. MATERIALS AND METHODS

### A. Experimental Methods

An experiment was conducted in citrus orchards under commercial management practices in Seville, Spain. One of the orchards was subjected to four irrigation treatments to obtain a gradient in a physiological status. Airborne imagery was collected in 2010 using an unmanned aerial vehicle (UAV) designed to carry thermal and hyperspectral sensors [7] (see Fig. 1). Water potential, stomatal conductance, and chlorophyll fluorescence differed in each treatment (details can be found in [7]). Field measurements of water status were conducted with a pressure bomb (PWSC Model 3000, Soilmoisture Equipment Corporation, Goleta, CA, USA) to measure the xylem water potential ( $\psi$ ) on 40 trees. In addition, stomatal conductance ( $G_s$ ) was measured in ten trees using a leaf porometer (SC-1, Decagon Devices Inc., Pullman, WA, USA).

The hyperspectral imager on board the UAV was a micro-hyperspectral camera (micro-hyperspec VNIR model, Headwall Photonics, Fitchburg, MA, USA) flown in the spectral mode of 260 bands in the 400–885-nm region, 1.85-nm sampling interval, and 12-bit radiometric resolution, yielding 6.4-nm full-width half-maximum (FWHM) with a 25- $\mu$ m slit. Data acquisition and storage on board the UAV was set to 50 frames per second at 18 ms integration time. The flight was conducted at an average height of 575 m above the ground level and 75 km/h speed. The camera had an 8-mm focal length optic resulting in a 522-m swath with a pixel size of 40 cm. The flight was conducted in the solar plane to minimize directional effects. Radiometric calibration was performed

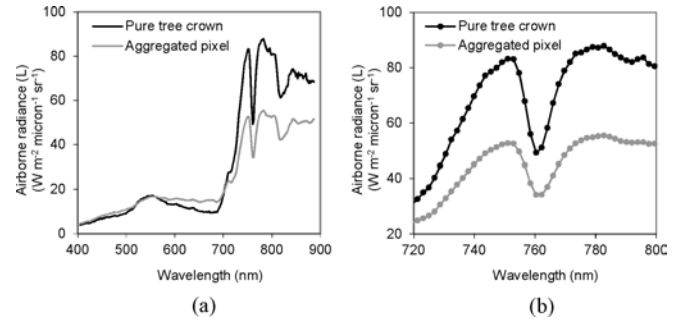


Fig. 2. (a) Airborne radiance (L) spectra extracted from pure tree crowns and aggregated pixels (including soil and shadows). (b) Observing the aggregation effects on the 15 spectral bands in the O<sub>2</sub>-A feature used for fluorescence quantification through the FLD3 method.

using coefficients derived from a calibrated integrating sphere (CSTM-USS-2000C LabSphere, North Sutton, NH, USA).

The hyperspectral imagery was atmospherically corrected based on total incoming irradiance (E) at 1-nm intervals simulated with the SMARTS model (see details in [7]). This was done using aerosol optical depth measured at 550 nm with a Micro-Tops II sunphotometer (Solar LIGHT Company, Philadelphia, PA, USA) collected in the study areas at the time of the flights. In addition, E was measured at the time of the flights using a 0.065-nm FWHM Ocean Optics HR2000 fiber-optic spectrometer (Ocean Optics, Dunedin, FL, USA), matching the spectral resolution of the airborne imagery through Gaussian convolution. Orthorectification was conducted with PARGE (ReSe Applications Schläpfer, Wil, Switzerland) using data from an inertial measuring unit installed on board the UAV and synchronized with the hyperspectral imager [see Fig. 1(a)]. The two central trees of each irrigation treatment block (a total of 32 trees) plus eight additional selected trees (40 trees in total) were used for extracting radiance (L), used to quantify F emission using the 760-nm O<sub>2</sub>-A in-filling method (see Fig. 2).

The fluorescence signal was quantified using the Fraunhofer line depth (FLD) method using three bands (FLD3) for both pure tree crowns and aggregated pixels including soil, shadows, and vegetation [see Fig. 2(a)]. In total, 15 spectral bands within the O<sub>2</sub>-A feature were observed in the radiance extracted [see Fig. 2(b)]. Fluorescence (F) was quantified using the  $L_{in}$  (L762),  $L_{out}$  (average of L747 and L780 bands),  $E_{in}$  (E762), and  $E_{out}$  (average of E747 and E780 bands) using [1]

$$F = \frac{E_{out} \cdot L_{in} - E_{in} \cdot L_{out}}{E_{out} - E_{in}}. \quad (1)$$

The F quantified on the trees of the experiment was compared with the field  $G_s$ , used here as a physiological indicator. In addition, the effects of pixel aggregation and percentage cover on the retrieval of the fluorescence signal were assessed for trees extracted in the entire flight line. In a very short distance, different planting grids and orientations were found [see Fig. 1(c)–(g)], showing a high variability of shadow components in trees of same species and similar sizes/shapes (see Fig. 3).

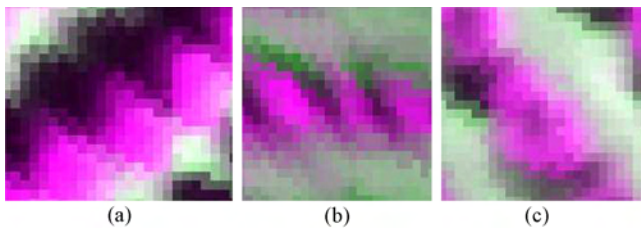


Fig. 3. (a)–(c) Complexity of the heterogeneous canopies under study, where extreme differences in the row orientation generate large effects on shadow proportions and sunlit components as a function of the sun angle. Images are shown in color composites using green, red, and NIR.

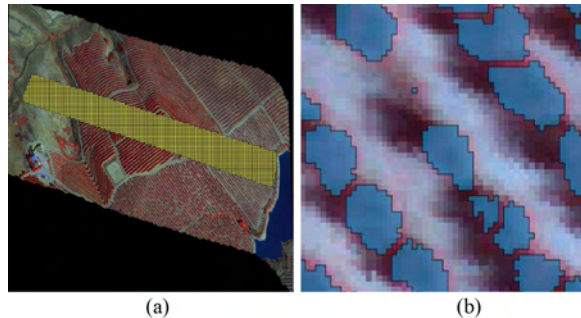


Fig. 4. (a) Nadir pixels selected for the quantification of  $F$  from pure-crown and aggregated pixels to avoid off-nadir angular effects. (b) Pure-crown pixel identification using the 40-cm hyperspectral image.

Fluorescence was also quantified from pure-vegetation pixels in the whole image (using the original 40 cm hyperspectral image [see Fig. 1(a)] and from aggregated pixels [see Fig. 1(b)] only in the nadir pixels of the flight line [see Fig. 4(a)] to avoid angular effects on the  $F$  assessment when off-nadir pixels were used. In addition, the fractional cover for each aggregated pixel was calculated through image segmentation using the original high-resolution image, quantifying the number of pure-vegetation pixels within each nadir pixel [see Fig. 4(b)]. From the nadir pixels selected, pure-crown and pixel-aggregated  $F$  were quantified through FLD3 to assess their relationship as a function of the fractional cover and assess the effects of the pixel mixture on the physiological measurements conducted.

### B. Modeling Methods

The assessment of canopy structural effects on fluorescence quantification was conducted using a leaf–canopy fluorescence model combined with a geometric model to account for canopy heterogeneity. Pure tree crown fluorescence was simulated with FluorMODleaf [14] combined with FluorSAIL [15], obtaining canopy radiance and reflectance from pure tree crown pixels with fluorescence effects (see [7] for further details). The coupled FluorMODleaf+FluorSAIL was combined with the forest light interaction model (FLIM) [17] to develop FluorFLIM for this letter. The aim was to assess the influence of scene components on the quantification of the fluorescence signal, retrieving fluorescence for a range of fractional covers in tree canopies. The FLIM model uses a first-order approximation of stand reflectance, considering the effects of crown transparency on apparent reflectance of shadowed soil background. From this approach, the canopy is

considered as a discontinuous canopy layer with crowns and gaps, with primary variability in stand reflectance due to variations in crown coverage, shadows, and crown transmittance. FluorFLIM uses crown reflectance (including fluorescence  $\rho_c$ ) from FluorMOD, generating canopy reflectance using inputs such as tree density  $T\delta$ , crown diameter  $Cd$ , crown height  $Ch$ , crown leaf area  $C_{LAI}$ , crown extinction coefficient  $C\alpha$ , sun angle  $\theta_s$ , and soil reflectance  $\rho_s$ . The method used here was a simple approximation due to the lack of current of more complex models to simulate  $F$  in nonhomogeneous canopies. There are several limitations to a more global application of this model to all types of heterogeneous canopies: 1) FLIM uses a random tree distribution with tree density and crown diameter to determine the percentage cover and therefore cannot be directly applied to all canopies and 2) FLIM does not include multiple scattering between crowns. Therefore, the methods used in this letter are a first attempt to highlight the importance of pixel-aggregation effects on  $F$  quantification until a more complex canopy model including fluorescence is developed. Our intention was not to conduct an exhaustive validation of the model. Instead, the FluorFLIM model developed in this letter was used to explore and simulate canopy scenes with input parameters within the typical range of variation observed in the field ( $Cd=3.5$  m,  $Ch=3$  m,  $C_{LAI}=5$ ,  $C\alpha=0.6$ ,  $\theta_s=65^\circ$ ), image-extracted  $\rho_s$ , and FluorMOD inputs to mimic the variation of  $F_{crown}$  found in this letter ( $N=1.8$ ;  $Cab=50 \mu\text{g cm}^{-2}$ ;  $Cw=0.02$ ;  $Cm=0.01$ ;  $T=15^\circ$ ;  $S=2$ ;  $Sto=2$ ; and  $F_i$  ranging between 0 and 0.1) (see [7] for further details on input parameters). Tree density  $T\delta$  was varied to generate a range between 30% and 90%, obtaining canopy L scenes with  $F$  [see Fig. 5(a)] to quantify  $F$  using the FLD3 method [see Fig. 5(b)] for each spectrum modeled as a function of percentage cover. These FluorFLIM simulations were then used to develop relationships between  $F_{crown}$  and  $F_{aggregated}$  pixels as a function of the % cover [see Fig. 5(c)] to estimate  $F_{crown}$  from pixel-aggregated  $F$  and percentage cover. The method was assessed in the nadir pixels of the image [see Fig. 4(a)] and the relationship between  $F_{crown}$  quantified from the high-resolution image and  $F_{crown}$  estimated from aggregated pixels was obtained.

### III. RESULTS

The  $F$  signal quantified from pure tree crowns in 40 trees of the experiment ranged between  $3.9$  and  $6.1 \text{ W m}^{-2} \mu\text{m}^{-1} \text{ sr}^{-1}$ . As expected, the fluorescence signal extracted from coarse resolution pixels showed a lower range, yielding between  $2.8$  and  $3.8 \text{ W m}^{-2} \mu\text{m}^{-1} \text{ sr}^{-1}$ . Due to the heterogeneity of the orchards in the tree dimension and density and to the interaction with Sun and observation geometry, which generate different shadow patterns, the relationship between fluorescence extracted from pure tree crown radiance and from aggregated pixel radiance was weak ( $R^2=0.25$ ;  $p<0.01$ ; see Fig. 6).

This result demonstrates the difficulties of interpreting the fluorescence signal calculated from aggregated pixels, especially in heterogeneous canopies with high variability in the percentage of scene components. Moreover, the canopy structure was shown to play a major role in quantified fluorescence due to the large effects caused by varying

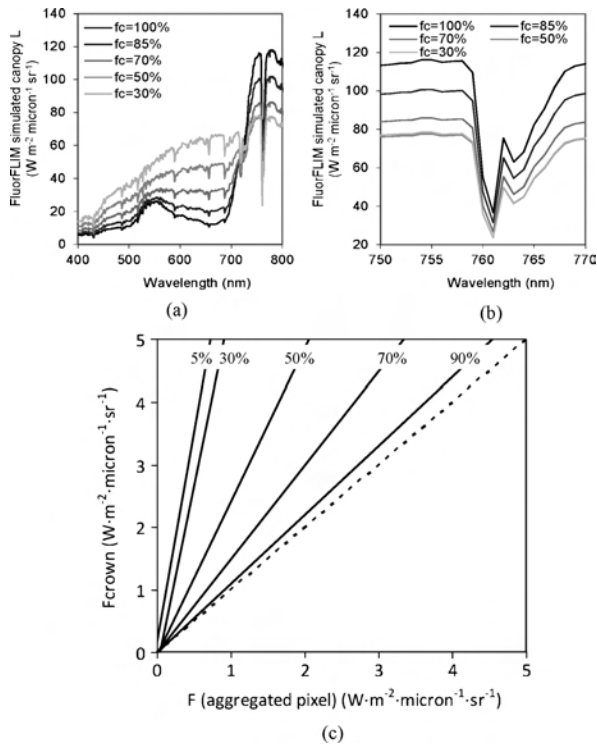


Fig. 5. (a) and (b) FluorFLIM simulations of canopy L for a range of percentage cover using pure-crown L obtained from FluorMOD and (c) used as prediction functions to estimate Fcrown from F aggregated pixels as a function of percentage cover.

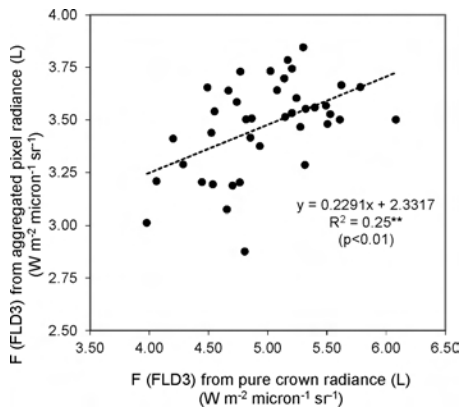


Fig. 6. Relationship obtained between the fluorescence signal quantified from pure tree crown airborne radiance (L) and from coarse resolution pixels. Statistical significance is shown as \*  $p < 0.05$ ; \*\*  $p < 0.01$ ; \*\*\*  $p < 0.001$ .

percentages of shadows and soil, masking changes in fluorescence amplitude caused by the physiological condition. This is of particular importance as chlorophyll fluorescence is intended as a link with canopy photosynthesis, and therefore associated with vegetation physiology. In this regard, relationships between stomatal conductance and chlorophyll fluorescence were also affected when using aggregated pixels (see Fig. 7). Similar results were found for water potential [7] (data not shown).

Results obtained between Gs and pure tree crown F ( $R^2 = 0.69$ ;  $p < 0.01$ ) indicated that F quantified from pure-vegetation radiance was a good indicator of physiological status, while aggregated pixel radiance obtained lower sensi-

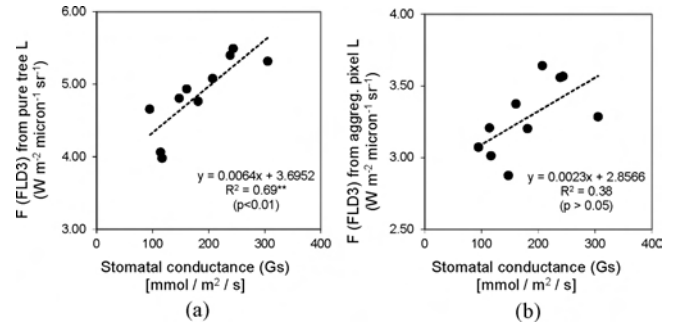


Fig. 7. Relationships obtained between stomatal conductance (Gs) and fluorescence (F) quantified through FLD3 from pure tree crown radiance (L) extracted (a) from the imagery and (b) from aggregated pixels. Statistical significance is shown as \*  $p < 0.05$ ; \*\*  $p < 0.01$ ; \*\*\*  $p < 0.001$ .

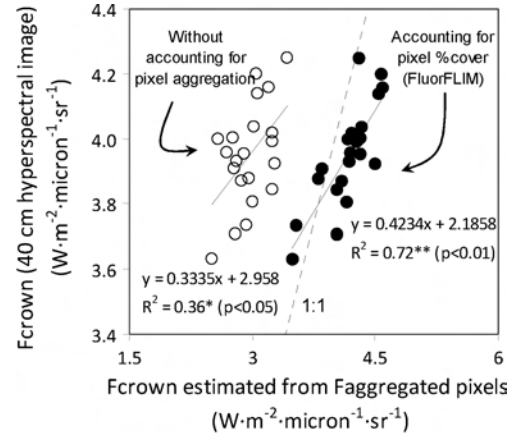


Fig. 8. Relationship between Fcrown (from the 40-cm image) and Fcrown estimated from coarse resolution using FluorFLIM functions. A weak relationship is obtained when no pixel-aggregation effects are considered. Statistical significance is shown as \*  $p < 0.05$ ; \*\*  $p < 0.01$ ; \*\*\*  $p < 0.001$ .

tivity ( $R^2 = 0.38$ ; statistically nonsignificant). This result was caused by the weak relationship obtained between Fcrown and F aggregated pixels (see Fig. 6). These experimental results agreed with FluorFLIM simulation results [see Fig. 5(c)]. In particular, the F signal quantified from the imagery in the nadir pixels and the simulations that generated scenes with the varying fractional cover showed large reductions in the signal when the fractional cover decreased from full cover.

The estimation of Fcrown from aggregated pixels using the FluorFLIM relationships [see Fig. 5(c)] was successful to a certain extent. In particular, the F signal quantified from aggregated pixels was weakly related to pure-crown F retrieval due to the large variation in the fractional cover (10–90% within the image;  $R^2 = 0.36$ ;  $p < 0.05$ ; see Fig. 8). But when Fcrown was estimated from FluorFLIM accounting for the fractional cover, the relationship greatly increased ( $R^2 = 0.72$ ;  $p < 0.01$ ) and approached 1:1. Nevertheless, Fcrown estimation errors were higher for pixels with low cover, deviating from the 1:1 line as shown in the figure.

#### IV. CONCLUSION

This letter is the first attempt to model the effects of vegetation structure on the fluorescence signal in heterogeneous

canopies. The aim was to make progress in the interpretation of fluorescence retrieved from aggregated pixels. High-resolution airborne hyperspectral imagery acquired at 40-cm pixel size over crop orchards made it possible to extract the radiance from pure tree crowns and pixels which included sunlit and shaded vegetation and soil components. Experimental results showed that the fluorescence signal calculated using the FLD3 method from aggregated image pixels was degraded, obtaining a weak relationship when compared against pure-crown fluorescence due to the effects of the varying fractional cover on each pixel ( $R^2=0.25$ ;  $p<0.01$ ). These effects due to the variation of the fractional cover in the quantification of F from coarse resolution pixels caused a lower sensitivity to physiological measures of vegetation physiology and stress such as stomatal conductance ( $R^2$  decreased from 0.69 to 0.38).

Exploratory simulations to confirm these experimental results were conducted with the FluorMOD model combined with FLIM to develop FluorFLIM for this letter. This combined simulation approach confirmed the important effects of percentage cover on the fluorescence signal retrieved from a coarser resolution. FluorFLIM simulations proved that the canopy cover may play a major role in the fluorescence signal measured in heterogeneous canopies. To account for these large effects of the fractional cover on F, FluorFLIM simulations were developed to estimate  $F_{\text{crown}}$  from F aggregated pixels. This modeling method enabled the estimation of  $F_{\text{crown}}$  from coarse resolution pixels when accounting for the fractional cover of each pixel ( $R^2=0.72$ ;  $p<0.01$ ). Nevertheless, larger errors in the estimation of  $F_{\text{crown}}$  were obtained in pixels with a low vegetation cover, which caused a slope that deviated from the 1:1 line.

These experimental and modeling results demonstrated that the simulation methods developed in this letter enabled the estimation of pure-vegetation fluorescence emission from aggregated pixels. The estimation of  $F_{\text{crown}}$  from coarse pixels is a critical issue as, in most cases, structural effects on fluorescence retrieval in mixed pixels may be greater than the typical variation of fluorescence (2–3% of radiance levels) caused by the physiological condition. This letter shows that a more refined canopy model including fluorescence is needed to better interpret the fluorescence signal in both closed and heterogeneous canopies, including row-structured planting grids and discontinuous canopies. The experimental and modeling results suggest that recently obtained global maps of chlorophyll F require information on pixel heterogeneity for a proper interpretation of the signal when quantified at global scales. If not considered, the gradients obtained for F as a function of fractional cover may show similar trends than standard vegetation indices (such as NDVI) due to the effects of fractional cover in mixed pixels. In addition to the assessment of the fractional cover conducted in this letter, further work will focus on the effects caused by the canopy architecture, including shadows and background effects, on the retrieval of the fluorescence signal from mixed pixels. Moreover, off-nadir and viewing geometry effects need attention when applying the methods discussed here to hyperspectral sensors flying on board manned and UAVs.

## REFERENCES

- [1] Z. Malenovsky, K. B. Mishra, F. Zemek, U. Rascher, and L. Nedbal, "Scientific and technical challenges in remote sensing of plant canopy reflectance and fluorescence," *J. Exp. Botany*, vol. 60, no. 11, pp. 2987–3000, 2009.
- [2] O. Pérez-Priego, G. Sepulcre-Cantó, J. R. Miller, J. Moreno, and E. Fereres, "Detection of water stress in orchard trees with a high-resolution spectrometer through chlorophyll fluorescence in-filling of the  $O_2$ -A band," *IEEE Trans. Geosci. Remote Sens.*, vol. 43, no. 12, pp. 2860–2869, Dec. 2005.
- [3] M. Meroni, V. Picchi, M. Rossini, S. Cogliati, C. Panigada, C. Nali, G. Lorenzini, and R. Colombo, "Leaf level early assessment of ozone injuries by passive fluorescence and PRI," *Int. J. Remote Sens.*, vol. 29, nos. 17–18, pp. 5409–5422, 2008.
- [4] M. Meroni, M. Rossini, V. Picchi, C. Panigada, S. Cogliati, C. Nali, and R. Colombo, "Assessing steady-state fluorescence and PRI from hyperspectral proximal sensing as early indicators of plant stress: The case of ozone exposure," *Sensors*, vol. 8, no. 3, pp. 1740–1754, 2008.
- [5] M. Meroni, M. Rossini, L. Guanter, L. Alonso, U. Rascher, and R. Colombo, "Remote sensing of solar-induced chlorophyll fluorescence: Review of methods and applications," *Remote Sens. Environ.*, vol. 113, no. 10, pp. 2037–2051, 2009.
- [6] I. Moya, L. Camenen, S. Evain, Y. Goulas, Z. G. Cerovic, G. Latouche, J. Flexas, and A. Ounis, "A new instrument for passive remote sensing 1. Measurements of sunlight-induced chlorophyll fluorescence," *Remote Sens. Environ.*, vol. 91, no. 2, pp. 186–197, 2004.
- [7] P. J. Zarco-Tejada, V. González Dugo, and J. A. J. Berni, "Fluorescence, temperature and narrowband indices acquired from a UAV platform for water stress detection using a micro-hyperspectral imager and a thermal camera," *Remote Sens. Environ.*, vol. 117, pp. 322–337, Feb. 2012.
- [8] L. Guanter, L. Alonso, L. Gomez-Chova, M. Meroni, R. Preusker, J. Fischer, and J. Moreno, "Developments for vegetation fluorescence retrieval from spaceborne high-resolution spectrometry in the  $O_2$ -A and  $O_2$ -B absorption bands," *J. Geophys. Res.*, vol. 115, no. D19, pp. 1–16, 2010.
- [9] A. Damm, A. Erler, W. Hillen, M. Meroni, M. E. Schaepman, W. Verhoef, and U. Rascher, "Modeling the impact of spectral sensor configurations on the FLD retrieval accuracy of sun-induced chlorophyll fluorescence," *Remote Sens. Environ.*, vol. 115, no. 8, pp. 1882–1892, 2011.
- [10] C. Frankenberg, J. B. Fisher, J. Worden, G. Badgley, S. S. Saatchi, J.-E. Lee, G. C. Toon, A. Butz, M. Jung, A. Kuze, and T. Yokota, "New global observations of the terrestrial carbon cycle from GOSAT: Patterns of plant fluorescence with gross primary productivity," *Geophys. Res. Lett.*, vol. 38, no. 17, pp. 1–6, 2011.
- [11] J. Joiner, Y. Yoshida, A. P. Vasilkov, Y. Yoshida, L. A. Corp, and E. M. Middleton, "First observations of global and seasonal terrestrial chlorophyll F from space," *Biogeosciences*, vol. 8, no. 3, pp. 637–651, 2011.
- [12] A. Kuze, H. Suto, M. Nakajima, and T. Hamazaki, "Thermal and near infrared sensor for carbon observation Fourier-transform spectrometer on the greenhouse gases observing satellite for greenhouse gases monitoring," *Appl. Opt.*, vol. 48, no. 35, pp. 6716–6733, 2009.
- [13] L. Guanter, C. Frankenberg, A. Dudhia, P. E. Lewis, J. Gomez-Dans, A. Kuze, H. Suto, and R. G. Grainger, "Retrieval and global assessment of terrestrial chlorophyll fluorescence from GOSAT space measurements," *Remote Sens. Environ.*, vol. 121, pp. 236–251, Jun. 2012.
- [14] R. Pedrós, I. Moya, Y. Goulas, and S. Jacquemoud, "Chlorophyll fluorescence emission spectrum inside a leaf," *Photochem. Photobiol. Sci.*, vol. 7, no. 4, pp. 498–502, 2008.
- [15] W. Verhoef, "Extension of SAIL to model solar-induced canopy fluorescence spectra," in *Proc. 2nd Int. Workshop Remote Sens. Vegetation Fluorescence*, Nov. 17–19, 2005, pp. 45–63.
- [16] M. Meroni, L. Busetto, R. Colombo, L. Guanter, J. Moreno, and W. Verhoef, "Performance of spectral fitting methods for vegetation fluorescence quantification," *Remote Sens. Environ.*, vol. 114, no. 2, pp. 363–374, 2010.
- [17] A. Rosema, W. Verhoef, H. Noorbergen, and J. J. Borgesius, "A new forest light interaction model in support of forest monitoring," *Remote Sens. Environ.*, vol. 42, no. 1, pp. 23–41, 1992.